articles

Involvement of striate and extrastriate visual cortical areas in spatial attention

A. Martínez[1], L. Anllo-Vento[2], M. I. Sereno[3], L. R. Frank[4], R. B. Buxton[4], D. J. Dubowitz[5], E. C. Wong[4,6], H. Hinrichs[7], H. J. Heinze[7] and S. A. Hillyard[2]

[1] Departments of Psychology, [2]Neurosciences, [3]Cognitive Science, [4]Radiology and [6]Psychiatry, University of California at San Diego, 9500 Gilman Drive, La Jolla, California 92093-0608, USA

[5] Division of Biology, California Institute of Technology, 200 East California Blvd., Pasadena, California, 91125 USA

[7] Dept. of Clinical Neurophysiology, Otto-von-Guericke University, Leipziger Strasse 44, Magdeburg, Germany

Correspondence should be addressed to S.A.H. (shillyard@UCSD.edu)

We investigated the cortical mechanisms of visual-spatial attention while subjects discriminated patterned targets within distractor arrays. Functional magnetic resonance imaging (fMRI) was used to map the boundaries of retinotopic visual areas and to localize attention-related changes in neural activity within several of those areas, including primary visual (striate) cortex. Event-related potentials (ERPs) and modeling of their neural sources, however, indicated that the initial sensory input to striate cortex at 50–55 milliseconds after the stimulus was not modulated by attention. The earliest facilitation of attended signals was observed in extrastriate visual areas, at 70–75 milliseconds. We hypothesize that the striate cortex modulation found with fMRI may represent a delayed, re-entrant feedback from higher visual areas or a sustained biasing of striate cortical neurons during attention. ERP recordings provide critical temporal information for analyzing the functional neuroanatomy of visual attention.

The panoramic scenes of the world contain more information than we can take in with a single glance. To examine the fine details of a visual scene, we must rely on the brain's capability to focus attention in a spatially selective manner and thereby facilitate the perception of stimuli within a restricted zone of the visual field[1,2]. This covert focusing of attention has been likened metaphorically to a 'spotlight'[3] or 'zoom lens'[4] that can be shifted to relevant locations even when the eyes remain stationary. Psychophysical experiments have shown that stimuli falling within the spotlight of attention are detected and discriminated more rapidly and accurately than stimuli at unattended locations[1–4].

The brain system that controls the attentional spotlight consists of an interconnected network of cortical and subcortical structures that modulates incoming information in the visual pathways[5–7]. A fundamental question that remains unresolved, however, is exactly where along the visual processing pathway this afferent neural activity is first modulated (either enhanced or suppressed) by spatial attention. The preponderance of evidence to date from single-neuron recordings in monkeys[8,9] and from electrophysiological[10,11], blood-flow neuroimaging[12–16] and optical imaging[17] studies in humans indicates that neural responses to attended-location stimuli are enhanced in higher extrastriate cortical areas but not in the striate cortex itself.

Recent single-neuron experiments in monkeys[18–20] and preliminary reports of fMRI studies in humans (M. Worden & W. Schneider, *Soc. Neurosci. Abstr.* **22**, 729.7, 1996; S.P. Gandhi *et al.*, *ARVO Meeting Abstr.*, 1998) have raised the possibility that spatial-selective attention may influence striate cortex activity during tasks that involve difficult visual discriminations. In addition,

several neuroimaging studies have reported activation in or near striate cortex during discrimination tasks in nonselective (that is, active versus passive) designs[21–24]. In the present study, neural activity associated with spatially focused attention was localized to both striate and extrastriate visual areas that were positively identified by retinotopic mapping techniques[25]. ERPs recorded in the same task provided critical information about the time course of stimulus-selection processes in these cortical areas.

The spatial attention task used here required subjects to discriminate lateralized target stimuli surrounded by distractors in a 'cluttered' visual field. The stimuli were 3×3 arrays of crosses superimposed on a background checkerboard pattern (**Fig. 1a**) that were flashed with equal probability to either the right or left visual field in a random sequence at an average rate of two arrays per second. The central element of most (86%) of the arrays was an upright 'T', which was inverted in infrequent (14%) target arrays. The subject's task was to maintain fixation on a central arrow and to attend to the sequence of arrays in the visual field indicated by the arrow's direction. Detections of target arrays in the attended field were reported by a button press. Stimuli in the opposite field were to be ignored. The direction of the arrow, and thus the subject's direction of attention, alternated every 20 seconds between the left and right visual field during experimental runs lasting three minutes.

Blood oxygen level-dependent (BOLD)-weighted fMRI images were acquired during task performance from ten contiguous slices extending anteriorly from the occipital pole. Attention effects over the entire group were obtained by transforming each individual's image set into standard Talairach coordinates[26]
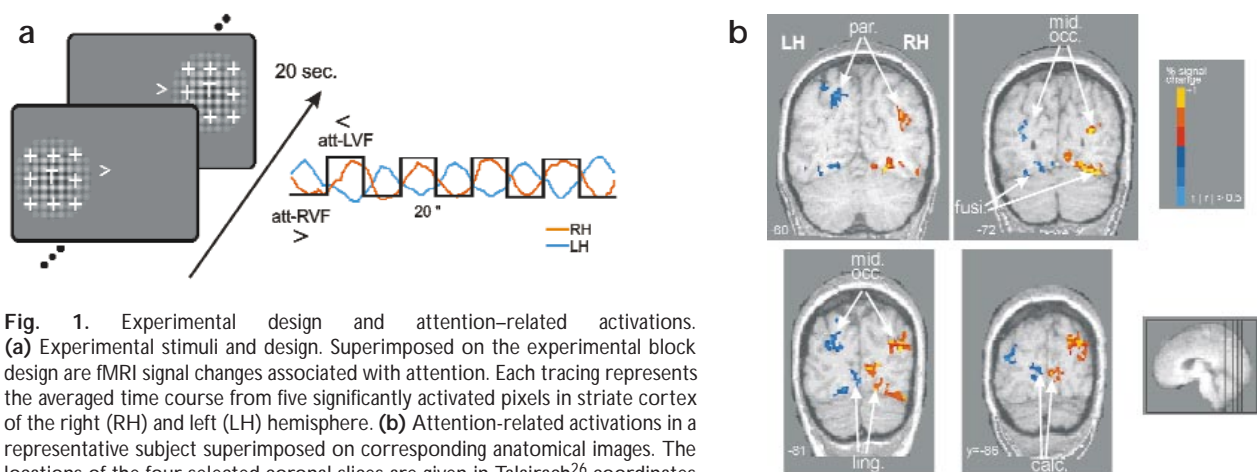
Fig. 1. Experimental design and attention–related activations. **(a)** Experimental stimuli and design. Superimposed on the experimental block design are fMRI signal changes associated with attention. Each tracing represents the averaged time course from five significantly activated pixels in striate cortex of the right (RH) and left (LH) hemisphere. **(b)** Attention-related activations in a representative subject superimposed on corresponding anatomical images. The locations of the four selected coronal slices are given in Talairach[26] coordinates (*y*-values). The left hemisphere appears on the left in all images. Intensity of colored regions reflects percentage signal change (difference between signal during attend-right and attend-left divided by the total signal) of significantly activated areas. Pixels with a time course of activation positively correlated with the task design (that is, showing greater activation during attention to the left visual field) are shown in the red-to-yellow scale. Those with a time course negatively correlated with the design (that is, showing greater activation during attention to the right visual field) are displayed in the dark-to-light blue scale. Only pixels correlating at $r > \pm 0.5$ ($p < 0.02$, corrected) are shown. Spatial attention produced contralateral activation foci in the calcarine fissure (calc.), lingual gyrus (ling.), posterior fusiform gyrus (fusi.), middle occipital gyrus (mid. occ.) and posterior parietal lobe (par.).

and averaging the time series of the BOLD signal for each co-registered pixel. Functional maps of brain activity related to the direction of attention were generated by cross-correlating each pixel of this group-averaged time series with a model reflecting the alternating block design of the experiment[27].

RESULTS

Subjects correctly detected an average of $81 \pm 7\%$ of the targets in the attended visual field. Significant increases in the BOLD signal (reflecting increases in regional cerebral blood flow, rCBF, and hence in neural activity[28]) were observed in several posterior cortical areas in the hemisphere contralateral to the attended visual field (**Fig. 1b**). These included the region of the calcarine fissure (which contains the striate cortex), the lingual, middle occipital and fusiform gyri, and the posterior parietal cortex. To identify the specific visual areas in which these rCBF changes occurred, the cortical surface of each subject was reconstructed and unfolded, and retinotopic areas were mapped onto the flattened surface[25]. Attention-related activations for individual subjects were

then projected onto their retinotopic maps (**Fig. 2**).

In all subjects, the boundaries of the retinotopic visual areas V1, V2, V3, VP, V3A and V4v could be clearly identified (**Fig. 2**). Attention-related increases in rCBF in the hemisphere contralateral to the attended visual field were observed in all subjects in area V1 and in most subjects in areas V2, V3, VP and V4v (**Table 1**). These activations were found at parafoveal retinotopic locations in both dorsal and ventral cortical areas, corresponding to the stimulus position in the visual field. In addition, most subjects had significant activation in weakly retinotopic areas of the middle occipital gyrus anterior to V3A and in the posterior fusiform gyrus anterior to V4v, as well as in non-retinotopic posterior parietal cortex (**Fig. 2**).

To obtain converging evidence about the time course of this attention-related neural activity, in separate sessions we recorded ERPs time-locked to the attended and unattended stimulus arrays under identical task conditions. For both right and left visual field stimuli, the attended arrays elicited enlarged positive P1 (onset at 70–75 ms) and negative N1 (onset at 130–140 ms)

Table 1. Cortical regions activated by attention

Ventral	V1	V2	VP	V4v	fusi.	
RH	7, –88, 0 (6) [150 ± 18]	7, –78, –3 (5) [156 ± 10]	9, –74, –8 (5) [167 ± 10]	19, –70, –11 (4) [167 ± 18]	33, –61, –13 (4) [192 ± 18]	
LH	–9, –90, –5 (4) [180 ± 20]	–12, –79, –8 (6) [150 ± 18]	–16, –75, –7 (6) [156 ± 11]	–26, –76, –11 (5) [188 ± 16]	–31, –60, –11 (6) [211 ± 12]	
Dorsal	V1	V2	V3	V3A	mid. occ.	post. par.
RH	7, –89, 1 (6) [193 ± 15]	7, –84, 5 (3) [141 ± 16]	21, –88, 13 (5) [138 ± 8]	24, –81, 19 (2) [125 ± 7]	27, –75, 13 (4) [219 ± 13]	28, –49, 57 (3) [162 ± 11]
LH	–8, –91, 0 (6) [162 ± 20]	–10, –85, 0 (5) [151 ± 10]	–22, –85, 14 (5) [141 ± 9]	- - - (0)	–29, –75, 19 (5) [219 ± 11]	–29, –55, 50 (3) [150 ± 10]

Mean Talairach coordinates of fMRI activation clusters within each visual area in ventral (top) and dorsal (bottom) cortical divisions. Coordinates for clusters in the right (RH) and left (LH) hemispheres are given separately. The total number of subjects (of six) showing significant ($p < 0.02$, corrected) activation in each area is given in parentheses. The total brain volume activated within each area (in cubic mm) is shown in brackets ± the standard error of the mean.

components over contralateral occipital scalp areas (**Fig. 3a**), as in previous studies[10,11,29]. In contrast, spatial attention did not affect the amplitude of the earlier C1 component (onset at 50–55 ms). Repeated measures ANOVAs showed significant amplitude increases with attention for both early (72–104 ms) and late (104–136 ms) phases of the P1 ($F_{1,18} = 8.9$, $p < 0.01$ and $F_{1,18} = 39.4$, $p < 0.001$, respectively) and for the N1 ($F_{1,18} = 15.0$, $p < 0.002$), particularly over the contralateral scalp. The C1 was not significantly modulated by attention ($F_{1,18} = 3.6$, n.s.).

We compared the surface voltage topographies of the midline parieto-occipital C1 and the contralateral occipital P1 attention effects (attended minus unattended differences in early and late time windows; **Fig. 3b**). From these grand-average topographical data, the neural sources of the C1 and of the P1 attention effect were estimated by dipole modeling using the Brain Electrical Source Analysis (BESA) algorithm[30]. As in previous reports[10,29,31], a single dipole in each hemisphere within the calcarine fissure in or near the primary visual cortex accounted for the C1 component's voltage topography over the time interval of 50–80 ms (**Fig. 4**). Anatomical localization of dipolar sources was achieved by projecting the BESA dipole coordinates of the group-average model (**Fig 4a**) onto the MRIs of seven individuals following co-registration of the BESA sphere with the MRI images (**Fig. 4b**). Dipole positions were converted into Talairach coordinates and averaged across all subjects (**Fig. 4c**; see ref. 29 for details).The Talairach coordinates for the left hemisphere C1 dipole were –9, –85, 5 and for the right hemisphere dipole were 10, –85, 5, both within the calcarine fissure. In contrast, the P1 attention effect required two pairs of dipoles for accurate modeling of its early and late phases (**Fig. 4**); the first dipole pair in dorsal extrastriate cortex of the middle occipital gyrus (left hemisphere, –32, –90, 9; right hemisphere, 33, –90, 10) accounted for the P1 over the time interval 72–96 ms, and the second pair in the ventral fusiform area (left hemisphere, –36, –56, –11; right hemisphere, 37, –56, –11) accounted for the time interval 104–136 ms.

Discussion

The fMRI data reported here provide direct evidence for the involvement of specific, retinotopically mapped visual cortical areas, including V1, V2, V3, VP and V4v, in spatial-selective attention. Whereas previous neuroimaging studies have shown activation of extrastriate visual areas in attention to location[12–16], the present finding of enhanced neural activity in retinotopically mapped striate cortex in a design that separates selective from non-selective attention effects has not been reported previously. This engagement of primary visual cortex may be attributed to our use of a difficult discrimination task that requires narrow focusing of the attentional spotlight in a cluttered visual field (M. Worden & W. Schneider *Soc. Neurosci. Abstr.* **22**, 729.7, 1996).

Our combined ERP and fMRI measurements have implications for the specific mechanisms by which attention to location modulates visual information processing in these cortical areas. Intriguingly, no attention-related changes were observed in the amplitude of the short-latency C1 component that reportedly represents the initial afferent response evoked in V1 by visual stimuli[29,31], despite the fMRI evidence that spatial attention was associated with increased neural activity in area V1. Although the neural generators of surface-recorded ERPs cannot be localized with the same degree of certainty as can hemodynamic changes using fMRI, the localization of the C1's dipole to the calcarine fissure, as well as its short onset latency (50 ms) and its retinotopic properties[10,31], are strongly indicative of a source in
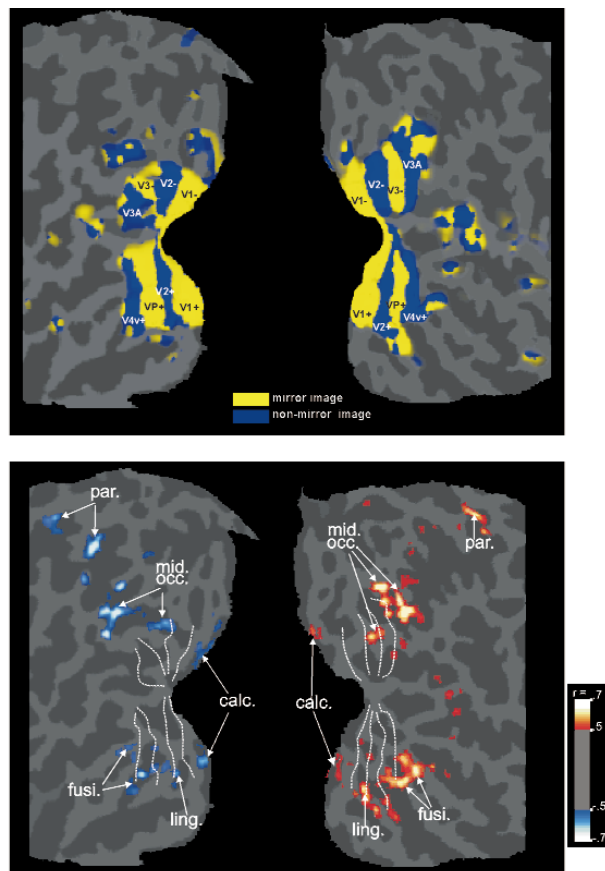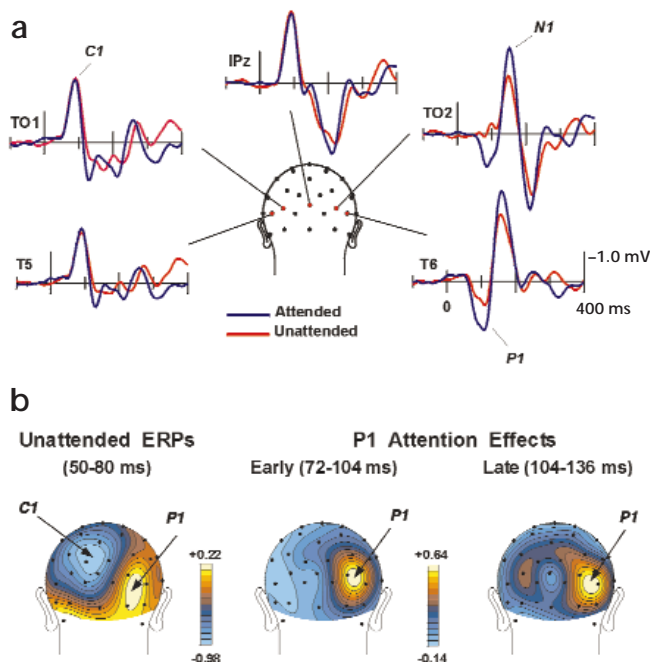

Fig. 2. Retinotopically mapped visual areas and co-localized attentional activations. Retinotopic visual areas (top) and regions of increased neural activity during spatial attention (bottom) mapped onto flattened cortical representations of the left (LH) and right hemispheres (RH) for the same subject shown in **Fig. 1b**. Sulcal cortex, dark gray; gyral cortex, light gray. Retinotopic (blue and yellow) areas representing upper (+) and lower (–) visual fields are located ventrally and dorsally, respectively. Uncolored areas include retinotopic areas representing unstimulated parts of the visual field (beyond six degrees of eccentricity) as well as non-retinotopic visual areas. Attention-related activations (bottom) were determined by cross-correlating pixel time courses with the task block design model; positive correlations (red scale) indicate increased neural activity during attend-left conditions and negative correlations (blue scale) increased activity during attend-right. Only pixels correlating at $r > 0.5$ ($p < 0.02$, corrected) are displayed. Dotted white lines on activation maps are boundaries of visual areas traced from field sign maps (top). Abbreviations of cortical regions are as in **Fig. 1**. The middle occipital (mid. occ.) region included the superior and inferior divisions of the middle occipital gyrus and associated sulci (lateral occipital and lunate).

area V1. Accordingly, these ERP findings argue against the hypothesis that spatial attention modulates the initial passage of visual input from the lateral geniculate nucleus through area V1 (refs. 32, 33), even under these cluttered field conditions.

If the modulation of activity in V1 found with fMRI does not represent a change in the initial geniculostriate input, what then is the role of the striate cortex in spatial attention? One hypothesis that draws support from both animal[19,20] (A.D. Mehta *et al., Soc. Neurosci. Abstr.* **23**, 121.1, 1997) and human[34] studies is that attentional modulation of striate activity occurs with a longer latency than the initial evoked response in striate cortex, and represents a delayed or re-entrant feedback of enhanced visual signals

Fig. 3. Grand-averaged ERP waveforms and scalp topographies. **(a)** ERP waveforms averaged over all subjects in response to standard (non-target) stimuli in the left visual field. Equivalent waveforms were elicited by right visual field stimuli. Recordings shown are from electrodes at occipitotemporal (TO1/TO2), temporal (T5/T6) and occipitoparietal (IPz) sites. Other sites are indicated as dots on the head icon. **(b)** Spline-interpolated voltage maps derived from the grand averaged waveforms shown in **(a)**. Color scales are in microvolts. Left map shows voltage topography averaged over the time window 50–80 ms for the unattended ERPs to left visual field stimuli. Distinctive C1 and P1 distributions are evident. Center and right maps show the distributions of the early and late P1 attention effects as manifested in the difference waves formed by subtracting the ERP to standard left visual field stimuli when unattended from the ERP to the same stimuli when attended.

back into V1 from higher extrastriate areas. Such a delayed attention effect was not evident in the present ERP recordings, but it could have escaped detection if the striate cortex source were weak enough to be masked by the stronger sources that were concurrently active in extrastriate cortex. An alternative hypothesis would be that the V1 activity observed during attention with fMRI represents a top-down 'bias' signal that produces a sustained increase in neural activity in V1 but does not modulate the initial stimulus-evoked response (for example, refs. 8, 35). Further work is needed to distinguish among these alternative mechanisms.

The ERP results indicate that the earliest facilitation of attended inputs occurs at a level beyond the striate cortex starting at 70–75 ms after the stimulus (after the onset of the P1 attention effect). The calculated source of this early facilitation was near the dorsal occipital foci of fMRI activation in area V3 and more anterior regions of the middle occipital gyrus. Similar dorsal sources for the P1 attention effect have been reported in studies that presented stimuli to the lower[14] but not upper[29,36] visual fields, suggesting that this early facilitation occurs in retinotopically organized extrastriate areas. In contrast, the source of the later phase of the P1 effect (104–136 ms) was situated in ventral

occipital cortex in the region of area V4v and posterior fusiform gyrus; this activity may be attributed to enhanced processing of the visual target information in ventral areas specialized for pattern and object recognition[11,13,27,36]. The activation foci observed in parietal cortex most likely reflect the engagement of the attentional control network that orchestrates the facilitation of attended inputs in extrastriate visual cortex[1,6,7].

In sum, these experiments provide evidence that the primary visual cortex is involved in spatial attention, but this area does not serve as the locus of initial sensory gain control where attended visual inputs are first selectively enhanced. This essential function of 'attentional amplification'[5], which improves the perceptibility of stimuli at attended locations, initially occurs in retinotopically organized extrastriate visual areas. These amplified signals are then routed to higher visual areas, including those of
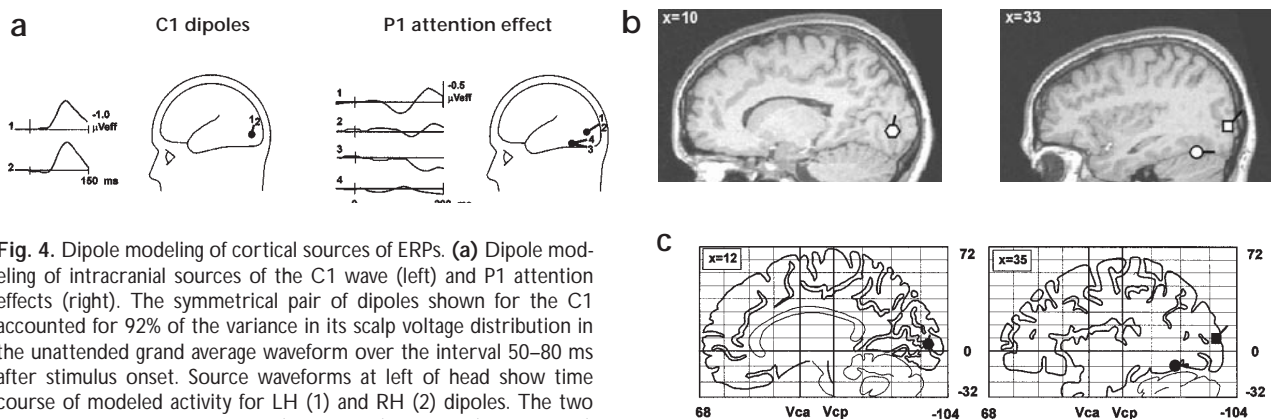

Fig. 4. Dipole modeling of cortical sources of ERPs. **(a)** Dipole modeling of intracranial sources of the C1 wave (left) and P1 attention effects (right). The symmetrical pair of dipoles shown for the C1 accounted for 92% of the variance in its scalp voltage distribution in the unattended grand average waveform over the interval 50–80 ms after stimulus onset. Source waveforms at left of head show time course of modeled activity for LH (1) and RH (2) dipoles. The two pairs of dipoles fitting the early (72–104 ms) and late (104–136 ms) phases of the P1 attention effects accounted for 94.8% of the variance of the scalp distribution of the grand average difference waves (attend minus unattend) over the interval 72–136 ms. Source waveforms are shown for the four P1 dipoles in response to left visual field stimuli: (1) early phase, right hemisphere, (2) early phase, left hemisphere, (3) late phase, right hemisphere, (4) late phase, left hemisphere. **(b)** Projections of calculated right-hemisphere dipolar sources of the C1 wave (left) and P1 attention effects (right) onto corresponding sagittal brain sections of an individual subject. Early P1 dipole, square; late P1 dipole, circle. **(c)** Projections of calculated dipolar sources averaged across subjects and projected on corresponding sections of the Talairach and Tournoux atlas[26].

articles

the occipitotemporal ventral stream, to gain preferential access to limited-capacity stages of feature analysis and pattern recognition. Bringing together the anatomical specificity of fMRI mapping and the time resolution of ERP recordings makes it possible to characterize the functional roles of specific brain areas in cognitive processes such as selective attention.

METHODS

fMRI procedures and data analysis. Six subjects (5 female, age range 23–41 years) gave written informed consent before participating in the fMRI experiment. Subjects were selected on the basis of their ability to maintain steady control of fixation as assessed by electro-oculographic recordings in pilot sessions. During fMRI scanning, eye movement was monitored continuously using an infrared-sensitive video camera system with a sensitivity of ± 0.5 degrees of visual angle. Runs with detectable eye movements were discarded and repeated.

The task stimuli were back-projected onto a screen at the foot of the magnet bore. Subjects viewed the stimuli via a mirror attached to the head coil. Each stimulus subtended 5.5 degrees of visual angle, and the innermost edge appeared 1.7 degrees to the left or right of fixation. Stimuli were presented in randomized sequences to either the left or right visual field with onset asynchronies varying between 400 and 600 ms. Stimulus duration was 100 ms.

Anatomical and functional images were acquired with a 1.5-T Siemens VISION MR scanner equipped with a 26 cm-diameter circularly polarized head coil. BOLD-weighted images were acquired with an echo planar imaging sequence (TR = 2500 ms, TE = 64 ms, flip angle = 90 degrees) in the coronal plane (2.5×2.5 mm in-plane resolution). Seventy-four repetitions on each of ten 5-mm slices were acquired during each three-minute run; the first two repetitions were not used in data analysis. For anatomical localization, high-resolution ($1 \times 1 \times 1$ mm) T1-weighted images were acquired using a three-dimensional magnetization-prepared rapid gradient echo sequence (TR = 11.4 ms, TE = 4.4 ms, flip angle = 10 degrees). Both anatomical and BOLD-weighted images were transformed into the standardized coordinate system of Talairach and Tournoux[26].

Time-dependent echo planar images were post-processed with AFNI software[37]. Following in-plane motion correction, the raw time-series data from each of four runs collected from every subject were averaged individually. Group data were obtained by averaging the time series over all subjects. A series of phase-shifted trapezoids representing the periodic alternation of conditions (attend-right, attend-left) in the block design of the experiment were used as reference waveforms. Each trapezoid function was correlated on a pixel-by-pixel basis with the averaged (individual or group) signal-strength time series by a least-squares fit to generate a functional intensity map. Gram–Schmitt orthogonalization was used to remove linear drift in the time series [27].

Significance levels of attention-related activations were determined by using a region of interest (ROI) analysis based on data from four pilot subjects. We identified anatomical regions of activation in these subjects and defined a single, large-volume ROI (28 ml) within the occipital cortex, which included the calcarine fissure, collateral sulcus, lingual gyrus and middle occipital gyrus. A conservative statistical correction (Bonferroni) based on the number of ROI voxels was applied for determining significance levels of attention-related activations in both individual and group data. These activations were considered significant for pixels correlating with the direction of attention at $r > 0.5$ (corrected $p < 0.02$).

Retinotopic mapping of visual areas. In a separate session, we obtained BOLD-weighted images while subjects viewed a slowly rotating checkerboard wedge and a dilating checkerboard circle. The periodic activations produced by these stimuli were used to calculate the borders of the retinotopically organized visual areas based on whether they contain a mirror-image, or non-mirror-image representation of the visual field (see ref. 25 for details).

ERP procedures and data analysis. ERPs were recorded during task performance from a group of 19 subjects (13 female, age range 18–41 years) including the 6 studied with fMRI. Recordings were made from 41 scalp

sites with an amplifier bandpass of 0.01–80 Hz. ERPs elicited by the same task stimuli as in the fMRI experiment were averaged separately according to field of stimulus and direction of attention, and grand-averaged over all subjects. Trials with eye movements or other artifacts were rejected off-line. ERP components were quantified as mean amplitudes in specific time windows relative to a 100-ms prestimulus baseline. Mean amplitudes of C1 (50–80 ms), P1 in its early (72–104 ms) and late (104–136 ms) phases, and N1 (150–180 ms) were analyzed by repeated-measures ANOVAs with factors of attention (same stimulus when attended and unattended), visual field (left and right), electrode site (20 pairs in each hemisphere) and hemisphere (left and right). Estimation of the dipolar sources of early ERP components was done using the BESA algorithm as described[29,38]. Modeling of the C1 component was done jointly on the waveforms elicited by unattended left and right visual-field standard stimuli (**Fig. 3a**). The interval between 50–80 ms was simultaneously with two dipoles, one in each hemisphere, that were constrained to have mirror-symmetrical locations and orientations. The attentional difference waves (attended minus unattended amplitudes) for left and right visual-field stimuli were used to fit the P1 attention effect. The early (72–104 ms) and late (104–136 ms) phases of the P1 were fitted sequentially, each with a pair of dipoles constrained to be mirror-symmetrical in location but allowed to vary in orientation. Different dipole-fitting strategies that included relaxing symmetry constraints and using different starting locations yielded highly similar dipole configurations.

1. LaBerge, D. *Attention Processing: The Brain's Art of Mindfulness* (Harvard Univ. Press, Cambridge, Massachusetts, 1995).
2. Luck, S. J., Hillyard, S. A., Mouloua, M. & Hawkins, H. L. Mechanisms of visual-spatial attention: Resource allocation or uncertainty reduction. *J. Exp. Psychol. Hum. Percept. Perform.* **22**, 725–737 (1996).
3. Posner, M. I., Snyder, C. R. & Davidson, B. J. Attention and the detection of signals. *J. Exp. Psychol. Gen.* **109**, 160–174 (1980).
4. Eriksen, C. W. & St. James, J. D. Visual attention within and around the field of focal attention: A zoom lens model. *Percept. Psychophysics* **40**, 225–240 (1986).
5. Posner, M. I. & Dehaene, S. Attentional networks. *Trends Neurosci.* **17**, 75–79 (1994).
6. Corbetta, M. Frontoparietal cortical networks for directing attention and the eye to visual locations: Identical, independent, or overlapping neural systems? *Proc. Natl. Acad. Sci. USA* **95**, 831–838 (1998).
7. Nobre, A. C. *et al.* Functional localization of the system for visuospatial attention using positron emission tomography. *Brain* **120**, 515–533 (1997).
8. Luck, S. J., Chelazzi, L., Hillyard, S. A. & Desimone, R. Neural mechanisms of spatial selective attention in areas V1, V2, and V4 of Macaque visual cortex. *J. Neurophysiol.* **77**, 24–42 (1997).
9. Colby, C. L. The neuroanatomy and neurophysiology of attention. *J. Child Neurol.* **6**, 90–118 (1991).
10. Mangun, G. R. Neural mechanisms of visual selective attention. *Psychophysiology* **32**, 4–18 (1995).
11. Hillyard, S. A. & Anllo-Vento, L. Event-related brain potentials in the study of visual selective attention. *Proc. Natl. Acad. Sci. USA* **95**, 781–787 (1998).
12. Heinze, H. J. *et al.* Combined spatial and temporal imaging of brain activity during visual selective attention in humans. *Nature* **372**, 543–546 (1994).
13. Mangun, G. R. *et al.* Covariations in ERP and PET measures of spatial selective attention in human extrastriate visual cortex. *Hum. Brain Mapp.* **5**, 273–279 (1997).
14. Woldorff, M. G. *et al.* Retinotopic organization of the early visual-spatial attention effects as revealed by PET and ERPs. *Hum. Brain Mapp.* **5**, 280–286 (1997).
15. Kastner, S., De Weerd, P., Desimone, R. & Ungerleider, L. Mechanisms of directed attention in the human extrastriate cortex as revealed by functional MRI. *Science* **282**, 108–111 (1998).
16. Mangun, G. R., Buonocore, M. H., Girelli, M. & Jha, A. ERP and fMRI measures of visual spatial selective attention. *Hum. Brain Mapp.* **6**, 383–389 (1998).
17. Gratton, G. Attention and probability effects in the human occipital cortex: An optical imaging study. *Neuroreport* **8**, 1749–1753 (1997).

18. Motter, B. C. in *The Attentive Brain* (ed. Parasuraman, R.) 51–69 (MIT Press, Cambridge, Massachusetts, 1998).

19. Roelfsema, P. R., Lamme, V. A. & Spekreijse, H. Object-based attention in the primary visual cortex of the macaque monkey. *Nature* **395**, 376–381 (1997).

20. Vidyasagar, T. R. Gating of neuronal responses in macaque primary visual cortex by an attentional spotlight. *Neuroreport* **9**, 1947–1952 (1998).

21. Shulman, G. L. *et al.* Top-down modulation of early sensory cortex. *Cereb. Cortex* **7**, 193–206 (1997).

22. Dupont, P. *et al.* Different perceptual tasks performed with the same visual stimulus attribute activate different regions of the human brain: A positron emission tomography study. *Proc. Natl. Acad. Sci. USA* **90**, 10927–10931 (1993).

23. Watanabe, T. *et al.* Attention-regulated activity in human primary visual cortex. *J. Neurophysiol.* **79**, 2218–2221 (1998).

24. Watanabe, T. *et al.* Task-dependent influences of attention on the activation of human primary visual cortex. *Proc. Natl. Acad. Sci. USA* **95**, 11489–11492 (1998).

25. Sereno, M. I. *et al.* Borders of multiple visual areas in humans revealed by functional magnetic resonance imaging. *Science* **268**, 889–893 (1995).

26. Talairach, J. & Tournoux, P. *Co-Planar Stereotaxic Atlas of the Human Brain: 3-Dimensional proportional system: An approach to cerebral imaging.* (Thieme, New York, 1988).

27. Bandettini, P. A., Jesmanowicz, A., Wong, E. C. & Hyde, J. S. Processing strategies for time-course data sets in functional MRI of the human brain. *Magn. Reson. Med.* **30**, 161–173 (1993).

28. Buxton, R. & Frank, L. A model for the coupling between cerebral blood flow and oxygen metabolism during neural stimulation. *J. Cereb. Blood Flow Metab.* **17**, 64–72 (1997).

29. Clark, V. P. & Hillyard, S. A. Spatial selective attention affects early extrastriate but not striate components of the visual evoked potential. *J. Cogn. Neurosci.* **8**, 387–402 (1996).

30. Scherg, M. in *Auditory Evoked Magnetic Fields and Electric Potentials* (eds. Grandori, F., Hoke, M. & Roman, G. L.) 40–69 (Karger, Basel, 1990).

31. Clark, V. P., Fan, S. & Hillyard, S. A. Identification of early visually evoked potential generators by retinotopic and topographic analysis. *Hum. Brain Mapp.* **2**, 170–187 (1995).

32. Crick, F. Function of the thalamic reticular complex: The searchlight hypothesis. *Proc. Natl. Acad. Sci. USA* **81**, 4586–4590 (1984).

33. Skinner, J. E. & Yingling, C. D. in *Attention, Voluntary Contraction and Event-Related Cerebral Potentials.* (ed. Desmedt, J. E.) 30–69 (Karger, Basel, 1977).

34. Aine, C. J., Supek, S. & George, J. S. Temporal dynamics of visual-evoked neuromagnetic sources: Effects of stimulus parameters and selective attention. *Int. J. Neurosci.* **80**, 79–104 (1995).

35. Rees, G., Frackowiak, R. & Frith, C. Two modulatory effects of attention that mediate object categorization in human cortex. *Science* **275**, 835–838 (1997).

36. Heinze, H. J., Luck, S. J., Mangun, G. R. & Hillyard, S. A. Visual event-related potentials index focused attention within bilateral stimulus arrays. I. Evidence for early selection. *Electroencephalogr. Clin. Neurophysiol.* **75**, 511–527 (1990).

37. Cox, R. W. AFNI—Software for analysis and visualization of functional magnetic resonance neuroimages. *Computers Biomed. Res.* **29**, 162–173 (1996).

38. Anllo-Vento, L., Luck, S. J. & Hillyard, S. A. Spatio-temporal dynamics of attention to color: Evidence from human electrophysiology. *Hum. Brain Mapp.* **6**, 216–238 (1998).